nature genetics

Wheat *Fhb1* encodes a chimeric lectin with agglutinin domains and a pore-forming toxin-like domain conferring resistance to Fusarium head blight

Nidhi Rawat[1,6], Michael O Pumphrey[2], Sixin Liu[3], Xiaofei Zhang[4], Vijay K Tiwari[1,6], Kaori Ando[2], Harold N Trick[5], William W Bockus[5], Eduard Akhunov[5], James A Anderson[4] & Bikram S Gill[1]

Fusarium head blight (FHB), caused by *Fusarium graminearum*, is a devastating disease of wheat and barley that leads to reduced yield and mycotoxin contamination of grain, making it unfit for human consumption. FHB is a global problem, with outbreaks in the United States, Canada, Europe, Asia and South America. In the United States alone, total direct and secondary economic losses from 1993 to 2001 owing to FHB were estimated at $7.67 billion[1]. *Fhb1* is the most consistently reported quantitative trait locus (QTL) for FHB resistance breeding. Here we report the map-based cloning of *Fhb1* from a Chinese wheat cultivar Sumai 3. By mutation analysis, gene silencing and transgenic overexpression, we show that a pore-forming toxin-like (*PFT*) gene at *Fhb1* confers FHB resistance. *PFT* is predicted to encode a chimeric lectin with two agglutinin domains and an ETX/MTX2 toxin domain. Our discovery identifies a new type of durable plant resistance gene conferring quantitative disease resistance to plants against *Fusarium* species.

Deploying disease-resistant cultivars is the most economical and durable method for controlling FHB in wheat, barley and other small grain crops, caused by *F. graminearum* species complex[2]. *Fhb1* (syn *Qfhs.ndsu-3BS*) derived from Chinese cultivar Sumai 3 is the most important quantitative trait locus (QTL) and has been reported to provide a moderately high level of genetic resistance against FHB[3,4]. *Fhb1* provides a broad-spectrum resistance against various isolates and species of *Fusarium*[5]. Several attempts have been made to identify the causal gene(s) at *Fhb1* by map-based cloning[6,7]. Various transcriptome-based searches to identify candidates of *Fhb1* have also been reported[8,9]. The 3.1-Mb *Fhb1* region of Chinese Spring (CS) chromosome 3B has been sequenced and studied extensively, but it does not have an active copy of the gene[10]. Association mapping based on the *Fhb1* region of CS did not delineate the candidate gene(s) for this QTL[11]. Isolation of this most important QTL for resistance to wheat scab remains a challenging task.

We report here the positional cloning of *Fhb1* from Chinese wheat cultivar Sumai 3. Previously, *Fhb1* had been narrowed down to a 0.08-cM region[6] in a set of high-resolution lines flanked by the DNA markers STS3B-355 and STS3B-334. We used these two flanking markers, other markers derived from CS 3BS, and BAC end-based markers to screen a Sumai 3 BAC library (**Supplementary Table 1**). We assembled eight overlapping BACs by fingerprinting. We sequenced four BACs (476D8, 71I24, 383G12 and 572D13) forming two contigs (~350 kb in total) with a physical gap in the *Fhb1* region, and assembled and annotated them. Thirteen genes were annotated on the Sumai 3 sequence (**Fig. 1**). Comparative analyses of *Fhb1* region of Sumai 3 with the publically available homoeologous regions of CS chromosomes 3B[10] (GenBank accession FN564434.1) and 3D[12] (GenBank accession HE774676.1) showed that its gene content and length of intergenic distances are more similar to 3D than 3B (**Fig. 1** and **Supplementary Table 2**). The physical gap was estimated to be ~76 kb and devoid of any new gene on the basis of comparison with CS 3D. The differences in gene content and length of intergenic spaces of CS 3B and Sumai 3 3B may be attributed to the higher rate of gene fragmentation and pseudogenization of CS 3B (**Fig. 1**) compared to CS 3D during evolution[12]. As expected, at the sequence level, the common genes and flanking sequences of Sumai 3 3B showed higher similarity with CS 3B than CS 3D (**Supplementary Table 2**). We observed no synteny of the Sumai 3 *Fhb1* region with rice, *Brachypodium*, sorghum and *Arabidopsis*.

To identify the major genetic determinant of FHB resistance, we performed expression analyses for the annotated genes using quantitative RT-PCR in spikes, inoculated with *Fusarium* macroconidia vs. water, of resistant near-isogenic line (R-NIL) with *Fhb1* and susceptible NIL (S-NIL) lacking the *Fhb1* locus[13]. The *PFT* and Nb-ARC domain-containing (*NBA*) genes were expressed only in R-NIL and not in S-NIL, whereas the other genes had similar expression patterns in both the NILs (**Supplementary Fig. 1**). Moreover, six genes of the thirteen had been ruled out previously by gene

[1]Wheat Genetics Resource Center, Department of Plant Pathology, Kansas State University, Manhattan, Kansas, USA. [2]Crop and Soil Sciences Department, Washington State University, Pullman, Washington, USA. [3]US Department of Agriculture–Agricultural Research Service, National Center for Cool and Cold Water Aquaculture, Kearneysville, West Virginia, USA. [4]Department of Agronomy and Plant Genetics, University of Minnesota, St. Paul, Minnesota, USA. [5]Department of Plant Pathology, Kansas State University, Manhattan, Kansas, USA. [6]Present address: Plant Sciences and Landscape Architecture Department, University of Maryland, College Park, Maryland, USA. Correspondence should be addressed to B.S.G. (bsgill@ksu.edu).

Received 18 November 2015; accepted 29 September 2016; published online 24 October 2016; doi:10.1038/ng.3706

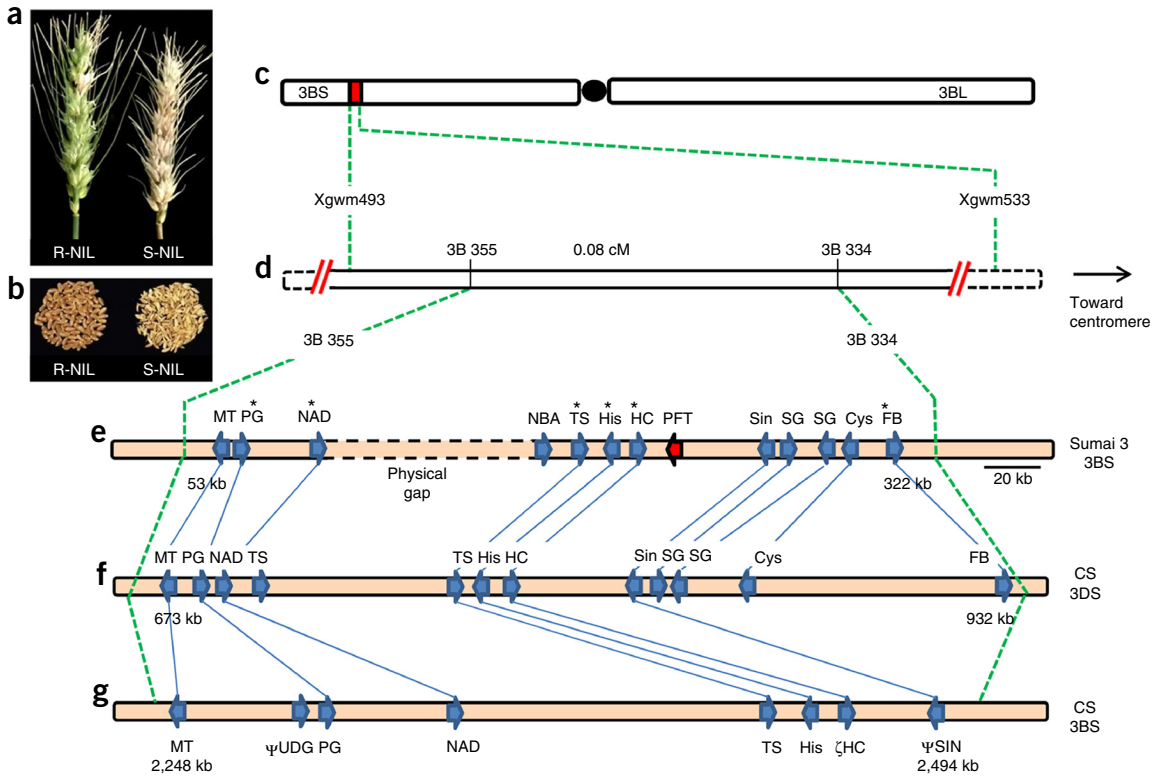

Figure 1 *Fhb1* phenotype and mapping. (**a**) Spikes of resistant and susceptible NILs showing difference in FHB phenotype. The S-NIL spike is severely bleached as compared to the green spike of R-NIL. (**b**) Shriveled and chalky *Fusarium*-damaged kernels of S-NIL compared with plump and healthy R-NIL seeds. (**c**) Chromosome location of the *Fhb1* region on 3BS of Sumai 3. (**d**) Genetic map of *Fhb1* delineated previously[6] by markers 3B 355 and 3B 334 to a 0.08-cM interval. (**e**) Physical map of *Fhb1* region of Sumai 3 containing 13 open reading frames (arrows) and their respective positions within the interval. Orange lines indicate repetitive regions without genes. Genes encoding the following proteins are marked: MT, tRNA methyl transferase; PG, polygalacturonase; NAD, oxidoreductase NAD binding; NBA, Nb-ARC domain containing; TS, terpene synthase; His, histidine-rich calcium-binding protein; HC, HCBT-like defense response protein; PFT, pore-forming toxin-like; Sin, Sina superfamily; SG, SGNH plant lipase; Cys, Cystatin; FB, F-box domain containing. Asterisks above the gene abbreviations mark the genes which were ruled out for *Fhb1* candidacy by transformation in previous studies[6,14]. (**f**) Comparison of homoeologous region in CS 3DS. (**g**) Comparison of homologous interval in CS 3BS. 'ζ' and 'ψ' denote gene fragment and pseudogene, respectively. ψUDG, pseudogene UDP-glucose 6-dehydrogenase. Accession numbers of proteins coded by the genes on 3BS and 3DS are provided in **Supplementary Table 8**.

complementation[6,14] (**Fig. 1e**). Of the seven remaining genes, *PFT* and *NBA* are known to have probable roles in plant defense[15,16], so we considered these two as the most promising candidate genes and studied them further for gene-structure and protein-sequence predictions.

We obtained full-length cDNA and complete genomic sequences for *PFT* and *NBA*, and analyzed them for gene structures. *NBA* is a 345-bp, single-exon gene predicted to encode a 114–amino acid protein with a partial NB-ARC domain and lacking other essential domains (coiled coil, Toll and interleukin-1 receptor, or leucine-rich repeat) characteristic of plant-disease-resistance proteins. Furthermore, in an association panel comprising landraces and cultivars known to vary for the presence of *Fhb1*, *NBA* was present in a susceptible haplotype containing cultivars Nanda 2419, Jingzhou 1 and Emai 6. Full-length sequencing of *NBA* in these four susceptible cultivars identified no amino acid change as compared to Sumai 3 (**Supplementary Table 3**). Therefore, we excluded *NBA* and considered *PFT* as the putative candidate for *Fhb1*.

PFT is a 3,472-bp gene with two exons generating a 1,437-bp mRNA. Random amplification of cDNA ends (RACE) showed *PFT* transcripts to have a 49-bp, 5′ untranslated region (UTR) and a 216-bp, 3′ UTR (**Fig. 2a**). The predicted protein was 478 amino acids, with two agglutinin domains and an ETX/MTX2 domain (**Fig. 2b**). *PFT* was expressed constitutively in the R-NIL (260-1-1-2), and its expression was the highest in pre-emerging spikes, after which we observed a sharp decline in transcript levels (**Supplementary Fig. 2**). The S-NIL (260-1-1-4) did not express the gene because it is null for *PFT*.

We assessed the candidacy of *PFT* for *Fhb1* using targeting induced local lesions in genome (TILLING) approach, RNA interference (RNAi)-induced gene silencing, association mapping and gene complementation by transformation. We screened a TILLING population made from an *Fhb1*/*Fhb1* resistant line HR58 (ref. 13) for mutations in the predicted agglutinin and ETX/MTX2 domains of *PFT*. Out of 1,929 M_2 families screened, we found 30 mutants, including two truncating, ten missense, one intronic and 17 silent mutations (**Supplementary Table 4**). The mutant pft^{1284} was a G>A transition, changing a tryptophan codon to a stop codon at position 233 located in the agglutinin domain. Another mutant pft^{1958} had a premature stop codon at position 361 located in the ETX/MTX2 domain. Missense mutants pft^{1409} (p.Ser226Phe) and pft^{1700} (p.Gly129Arg) caused amino acid changes in the protein. Mutant pft^{528} had a G>A transition 4 bp upstream of exon 2, which led to aberrant splicing in the mRNA. These five mutations in homozygous state caused the plants to be susceptible to FHB (**Fig. 2a** and **Supplementary Table 4**). Visually, the spikes of susceptible mutants were severely bleached after infection, whereas those of HR58 parent were green (**Fig. 2c**). They also had substantially higher deoxynivalenol (DON) content and a

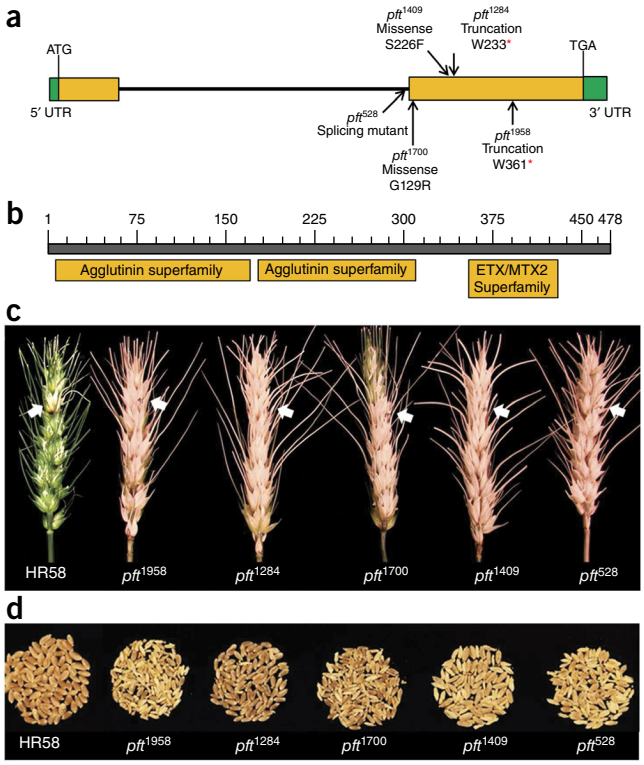

Figure 2 Gene structure and mutant analysis of *PFT*. (**a**) The *PFT* gene has two exons (orange boxes) connected by an intron (connecting black line). Green boxes at both the ends show the 5′ and 3′ untranslated region. Arrows indicate positions of the susceptible TILLING mutations. (**b**) Conserved domain analysis of the PFT protein showing two agglutinin superfamily domains and an ETX/MTX2 superfamily domain. Gray box depicts the protein with numbers marking amino acid positions. The analysis was conducted using NCBI conserved domain search tool. (**c**) FHB-infected spikes of susceptible TILLING mutants showing severe bleaching contrasting with the green spikes of parent HR58. White arrows point to the inoculation sites. (**d**) Shriveled and chalky fusarium damaged kernels of the mutants as compared with the healthy and plump seeds of resistant parent HR58.

higher percentage of shriveled, chalky and visually scabby kernels than the controls HR58 and R-NIL (**Fig. 2d** and **Supplementary Table 4**). Resequencing of exons of all the other genes in the *Fhb1* region in the susceptible mutants (using primers listed in **Supplementary Table 1**) revealed no mutations, including in *NBA*, confirming that the unique mutations in *PFT* were responsible for the loss of resistance to FHB in these plants.

For RNAi-induced gene silencing, we introduced an RNAi construct of *PFT* into the wheat cultivar Bobwhite, which is amenable to transformation but does not have *Fhb1* (**Fig. 3a**). Sumai 3 and the R-NIL with *Fhb1* were not amenable to tissue culture and, thus, were not responsive to transformation. F_1 plants from reciprocal crosses of the R-NIL and Bobwhite (non-transformed) were resistant to FHB (**Fig. 3b**). Five of ten F_1 R-NIL-RNAi Bobwhite plants showed the presence of both the RNAi construct and the *PFT* gene, and were highly susceptible to FHB (**Fig. 3b–d**). The number and phenotypes of spikes tested for the plants in this experiment are provided in **Supplementary Table 5**. Quantitative PCR showed the expression of *PFT* to be reduced by at least 150-fold in the spikes of five R-NIL-RNAi F_1 plants compared to F_1 R-NIL-Bobwhite plants (**Fig. 3e**).

We sequenced the 13 genes from the *Fhb1* region in an association mapping panel of 40 wheat landraces and cultivars known to differ for their FHB phenotype[7,17] (**Supplementary Table 3**). One resistant and four distinct susceptible haplotypes were visible in the region (**Supplementary Table 6**). Among the 40 wheat genotypes in the panel, all *Fhb1* resistant lines carried the *PFT* gene. Among the susceptible genotypes, 15 genotypes belonging to haplotypes S1, S2 and S4 were null for *PFT*, whereas three genotypes comprising haplotype S3 carried the same two SNPs each in the *PFT* gene. One SNP was a silent change and the second SNP caused aberrant splicing of mRNA as found in the susceptible TILLING mutant pft^{528}, confirming that *PFT* is necessary for FHB resistance (**Supplementary Fig. 3**).

To determine whether *PFT* is sufficient to confer resistance against FHB, we generated transgenic plants expressing the *PFT* gene under the control of maize ubiquitin promoter in hexaploid wheat cultivars Bobwhite and Fielder. Of the 11 T_0 plants, four (#7879, #7636, #7993, and #7978) showed expression of the transgene (**Supplementary Fig. 4**). We tested T_1 families from two independent transgenic events, #7879 (Bobwhite) and #7978 (Fielder) having healthy and fertile plants for the expression of the gene and FHB disease progress and resistance. The transgene segregated as a single gene in both the families. The T_1 plants showing expression of *PFT* were found to be either resistant or have considerably slower progress of the disease than untransformed controls (**Supplementary Fig. 5** and **Supplementary Table 7**), whereas the plants lacking the transgene expression were similar in their susceptibility to the untransformed controls. Levels of resistance were variable in different plants within the same family. This could be due to differences in the levels of expression of transgene in different plants, zygosity of transgene (hetero or homo), or the possibility that some background gene(s) may be required for complete expression of resistance conferred by *Fhb1*.

DON, the toxin associated with FHB, is known to be glucosylated to nontoxic deoxynivalenol-3-*O*-glucoside (D3G) in wheat plants[18], and the ability to detoxify DON has been reported to co-localize with *Fhb1* in wheat[19]. To test whether *PFT* has a role in the detoxification, we injected the middle spikelets of spikes of the NILs, knockout mutant lines and line HR58 with purified DON, and measured the amount of DON and D3G at 1, 3, 7, 14 and 21 d after inoculation. Visually, the S-NIL spikes were severely bleached above the point of injection, whereas the spikes of the R-NIL, HR58 and the truncation mutants did not have any bleaching (**Supplementary Fig. 6**), indicating that the DON-detoxification-controlling locus is independent of *PFT* but is located near the same genetic block. DON was converted to D3G in all the lines in the inoculated middle spikelets, whereas the terminal and basal spikelets had negligible DON and D3G content. The D3G:DON ratios in the middle spikelets were significantly lower in the S-NIL compared to that in the R-NIL, up to 7 d after inoculation ($t_2 = 0.038$, $P < 0.05$), after which the ratios were similar in both lines (**Supplementary Fig. 6**). The mutants, however, were not different from the R-NIL and HR58 in their D3G:DON ratio, indicating that *PFT* does not have a role in the detoxification of DON. The expression of numerous glucosyl transferases in wheat increases upon DON inoculation[20,21]. Seven glycosyl transferases (functional or nonfunctional) have been annotated in the 3.1-Mb CS contig (GenBank accession FN564434) containing the *Fhb1* region of Sumai 3 (ref. 10). The glucosyl transferase(s) near the *Fhb1* genetic block in the R-NIL may be assisting in the initial faster detoxification of DON compared to the S-NIL.

The predicted PFT protein is a chimeric lectin with two domains homologous to *Amaranthus caudatus* agglutinin and a bacterial ETX/MTX2 family domain (**Fig. 2b**). Plant lectins are a heterogeneous group of proteins of diverse origin that reversibly bind to carbohydrates and have been reported to play a role in plant defense against insects, nematodes, bacteria, fungi and viruses[15]. Chimeric lectins are

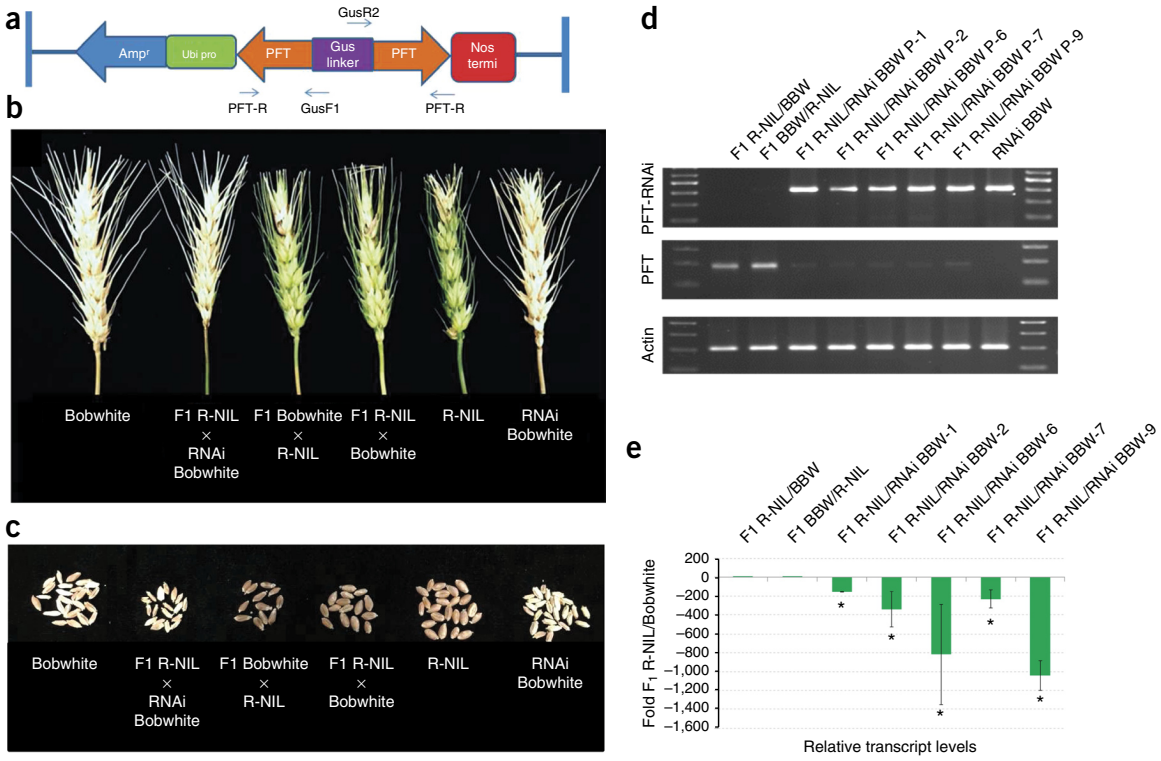

Figure 3 Functional validation of *PFT* with RNAi-induced gene silencing. (**a**) Structure of the self-complementary RNAi construct of *PFT* used in the transformation experiments. Expression of the construct was driven by maize *Ubiquitin* promoter. (**b**) *Fusarium*-infected bleached spikes from the RNAi cross as compared to green spikes of crosses without the RNAi construct. The spikes of F1 R-NIL × RNAi Bobwhite plant were severely bleached similar to the susceptible parents Bobwhite and RNAi Bobwhite, whereas spikes of resistant parent R-NIL and F1 plants without the RNAi construct (spikes in the middle) were green. Black dots on the spikes mark the points of inoculation. (**c**) *Fusarium*-damaged kernels of an RNAi cross plant as compared to plants without the RNAi construct. The seeds of F_1 R-NIL × RNAi Bobwhite plants were shriveled and chalky, characteristic of visually scabby kernels, as compared to the healthy seeds of R-NIL and F_1 plants without the RNAi construct (kernels in the middle stacks). (**d**) Reverse transcription PCR detected RNAi construct only in the transgenic lines (top gel); *PFT* was expressed in non-transgenic control but was suppressed in RNAi lines (middle gel). Actin confirmed the presence of mRNA in all the samples (bottom gel). (**e**) Quantitative PCR in spikes of F_1 plants at pre-anthesis stage showed at-least 150-fold reduction in plants with the RNAi construct as compared to F_1 plants without the RNAi construct. Error bars, s.d. ($n = 12$). $^*P < 0.01$ (significant), Student's *t* test.

composite proteins that have other domains, in addition to the basic agglutinin domains, with important biological functions. BLAST searches with the predicted PFT protein sequence showed high similarity to proteins in diverse plants, both dicots and monocots, ranging from *Aegilops tauschii* and *Brachypodium distachyon* to *Vitis vinifera*, *Jatropha curcus* and *Cucumis sativus* (**Supplementary Fig. 7** and **Supplementary Table 8**), although we found no significant hits in *Arabidopsis* and rice. We found the highest level of similarity (76%) with a predicted protein of *Ae. tauschii* (GenBank accession EMT22646.1). No signal peptide was predicted in the deduced PFT protein sequence. The biochemical mechanism of PFT-mediated FHB resistance is still unknown. The carbohydrate specificity of lectins is known to confer their biological properties for plant defense against pathogens[15,22]. ETX/MTX2 proteins are shown to be potent bacterial toxins that form channels in the cell membrane of the host leading to its death[23,24]. Modeling of the tertiary structure suggested that PFT may participate in the recognition of fungus-specific carbohydrates and cause toxicity to the fungus. A protein in wheat (Hfr2) similar to PFT has been known to increase membrane permeability of the host to facilitate mineral transport to virulent Hessian fly larvae[25]. If the predicted PFT protein shares similar functionality with antifungal lectins and ETX/MTX2 proteins, it is possible that PFT could arrest fungal growth by interacting with the fungal wall. However, further studies are needed to understand the mechanism of PFT action.

The proposed action of PFT aligns with the durable, broad-spectrum nature of *Fhb1* resistance. The *Fhb1*-mediated resistance of wheat to *Fusarium* spp. is not a classic NBS-LRR-mediated gene-for-gene type of reaction. The durability of this gene is most probably because, unlike NBS-LRR proteins, it is not a receptor for fungal avr proteins, which rapidly evolve to overcome host R gene products. *Fhb1* provides resistance to a broad range of isolates and species of *Fusarium,* including *F. graminearum*, *F. culmorum*, *F. avenaceum*, *F. nivale* and *F. poae*[5,26]. In fact, *F. graminearum* has been reported to lack any pathogen specialization that induces gene-for-gene-mediated hypersensitive reaction in the host[27]. Furthermore, classic R genes that suffer boom-and-bust cycles could not have durably controlled the spread of *F. graminearum*, unlike the quantitative resistance of Sumai 3 *Fhb1*, which has remained a major source of durable resistance since its release in China in 1972 and further deployment worldwide[3,4,28]. Sequence information for the causal variation at *Fhb1* will be useful for designing perfect markers for marker-assisted breeding, gene pyramiding and genetic engineering to provide a long-term, economical solution to FHB disease.

METHODS

Methods and any associated references are available in the online version of the paper.

Accession codes. All sequences have been deposited in GenBank: KX907434.

Note: Any Supplementary Information and Source Data files are available in the online version of the paper.

ACKNOWLEDGMENTS

This work was supported by US Wheat and Barley Scab Initiative (USDA-ARS grant 59-0206-2-088) and US National Science Foundation grant contract (IIP-1338897). We thank G. Bai for (USDA-ARS, Manhattan, Kansas) providing seeds of wheat cultivars and landraces for association studies and S. McCormick (USDA-ARS, Peoria, Illinois) for providing purified DON for inoculation experiments. We thank A. Akhunova, R. Matniyazov, S. Sehgal, S. Simsek, K. Benson, B. Friebe, D. Wilson, J.W. Raupp, N. Tyagi, U.M. Quraishi and L. Jiarui for technical support. We acknowledge help from student workers C. McDaniel, K. Madden and R. Clay-Pettis. This is contribution 16-147-J from the Kansas Agricultural Experiment Station.

AUTHOR CONTRIBUTIONS

N.R. and M.O.P. performed most of the experimental work. S.L. developed the near-isogenic lines and markers for the initial part of the work. X.Z. carried out DON and D3G analyses, and additional phenotyping of the mutants. V.K.T. made the RNAi crosses and did their phenotyping. K.A. isolated some of the TILLING mutants. H.N.T. generated RNAi plants. W.W.B. produced inocula for all the phenotyping work. E.A. developed the BAC library and provided useful discussions. N.R., J.A.A. and B.S.G. conceived the research and co-wrote the manuscript.

COMPETING FINANCIAL INTERESTS

The authors declare no competing financial interests.

1. Nganje, W.E., Kaitibie, S., Wilson, W.W., Leistritz, F.L. & Bangsund, D.A. Economic impacts of *Fusarium* head blight in wheat and barley: 1993–2001 (Agribusiness and Applied Economics Report No. 538) (North Dakota State University, 2004).
2. McMullen, M., Jones, R. & Gallenberg, D. Scab of wheat and barley: a reemerging disease of devastating impact. *Plant Dis.* **81**, 1340–1348 (1997).
3. Jin, L.F. *et al. Fusarium* head blight resistance in U.S. winter wheat cultivars and elite breeding lines. *Crop Sci.* **53**, 2006–2013 (2013).
4. Anderson, J.A., Glover, K. & Mergoum, M. Successful adoption of spring wheat cultivars with moderate resistance to FHB by growers in the North Central Region. in *Proc. 2011 Natl.* Fusarium *Head Blight Forum* (eds. Canty, S., Clark, A., Anderson-Scully, A., Ellis, D. & Van Sanford, D.) 3 (US Wheat and Barley Scab Initiative, 2011).
5. Stack, R.W., Frohberg, R.C. & Casper, H. Reaction of spring wheats incorporating Sumai-3 derived resistance to inoculation with seven *Fusarium* species. *Cereal Res. Commun.* **25**, 667–671 (1997).
6. Liu, S. *et al.* Towards positional cloning of *Fhb1*, a major QTL for *Fusarium* head blight resistance in wheat. *Cereal Res. Commun.* **36**, 195–201 (2008).
7. Bernardo, A.N., Ma, H., Zhang, D. & Bai, G. Single nucleotide polymorphism in wheat chromosome region harboring *Fhb1* for *Fusarium* head blight resistance. *Mol. Breed.* **29**, 477–488 (2012).
8. Schweiger, W. *et al.* Transcriptomic characterization of two major *Fusarium* resistance quantitative trait loci (QTLs), *Fhb1* and *Qfhs.ifa-5A*, identifies novel candidate genes. *Mol. Plant Pathol.* **14**, 772–785 (2013).
9. Xiao, J. *et al.* Transcriptome-based discovery of pathways and genes related to resistance against *Fusarium* head blight in wheat landrace Wangshuibai. *BMC Genomics* **14**, 197 (2013).
10. Choulet, F. *et al.* Megabase level sequencing reveals contrasted organization and evolution patterns of the wheat gene and transposable element spaces. *Plant Cell* **22**, 1686–1701 (2010).
11. Hao, C. *et al.* Association mapping and haplotype analysis of a 3.1-Mb genomic region involved in *Fusarium* head blight resistance on wheat chromosome 3BS. *PLoS One* **7**, e46444 (2012).
12. Bartoš, J. *et al.* Intraspecific sequence comparisons reveal similar rates of non-collinear gene insertion in the B and D genomes of bread wheat. *BMC Plant Biol.* **12**, 155 (2012).
13. Liu, S. *et al.* Complex microcolinearity among wheat, rice, and barley revealed by fine mapping of the genomic region harboring a major QTL for resistance to *Fusarium* head blight in wheat. *Funct. Integr. Genomics* **6**, 83–89 (2006).
14. Pumphrey, M.O. *Towards Map-Based Cloning of* Fusarium *Head Blight Resistance QTL* Fhb1 *and Non-Additive Expression of Homoeologous Genes in Allohexaploid Wheat.* PhD thesis (Kansas State University, 2007).
15. Lannoo, N. & Van Damme, E.J.M. Lectin domains at the frontiers of plant defense. *Front. Plant Sci.* **5**, 397 (2014).
16. McHale, L., Tan, X., Koehl, P. & Michelmore, R.W. Plant NBS-LRR proteins: adaptable guards. *Genome Biol.* **7**, 212 (2006).
17. Yu, J.B., Bai, G.H., Zhou, W.C., Dong, Y.H. & Kolb, F.L. Quantitative trait loci for *Fusarium* head blight resistance in a recombinant inbred population of Wangshuibai/Wheaton. *Phytopathology* **98**, 87–94 (2008).
18. Berthiller, F. *et al.* Masked mycotoxins: determination of a deoxynivalenol glucoside in artificially and naturally contaminated wheat by liquid chromatography–tandem mass spectrometry. *J. Agric. Food Chem.* **53**, 3421–3425 (2005).
19. Lemmens, M. *et al.* The ability to detoxify the mycotoxin deoxynivalenol colocalizes with a major quantitative trait locus for *Fusarium* head blight resistance in wheat. *Mol. Plant Microbe Interact.* **18**, 1318–1324 (2005).
20. Lin, F.Y., Lu, Q.X., Xu, J.H. & Shi, J.R. Cloning and expression analysis of two salt and *Fusarium graminearum* stress associated UDP–glucosyltransferases genes in wheat. *Yi Chuan* **30**, 1608–1614 (2008).
21. Lulin, M. *et al.* Molecular cloning and characterization of an up-regulated UDP–glucosyltransferase gene induced by DON from *Triticum aestivum* L. cv. Wangshuibai. *Mol. Biol. Rep.* **37**, 785–795 (2010).
22. Van Damme, E.J.M., Lannoo, N. & Peumans, W.J. Plant lectins. *Adv. Bot. Res.* **48**, 107–209 (2008).
23. Thanabalu, T. & Porter, A.G. A *Bacillus sphaericus* gene encoding a novel type of mosquitocidal toxin of 31.8 kDa. *Gene* **170**, 85–89 (1996).
24. Petit, L., Maier, E., Gibert, M., Popoff, M.R. & Benz, R. *Clostridium perfringens* epsilon toxin induces a rapid change of cell membrane permeability to ions and forms channels in artificial lipid bilayers. *J. Biol. Chem.* **276**, 15736–15740 (2001).
25. Puthoff, D.P., Sardesai, N., Subramanyam, S., Nemacheck, J.A. & Williams, C.E. *Hfr-2*, a wheat cytolytic toxin–like gene, is up-regulated by virulent Hessian fly larval feeding. *Mol. Plant Pathol.* **6**, 411–423 (2005).
26. Mesterházy, Á. Role of deoxynivalenol in aggressiveness of *Fusarium graminearum* and *F. culmorum* and in resistance to *Fusarium* head blight. *Eur. J. Plant Pathol.* **108**, 675–684 (2002).
27. van Eeuwijk, F.A. *et al.* Assessing non-specificity of resistance in wheat to head blight caused by inoculation with European strains of *Fusarium culmorum*, *F. graminearum* and *F. nivale* using a multiplicative model for interaction. *Theor. Appl. Genet.* **90**, 221–228 (1995).
28. Bai, G.H., Chen, L.F. & Shaner, G. in Fusarium *Head Blight of Wheat and Barley* (eds. Leonard, K.J. & Bushnell, W.R.) 296–317 (American Phytopathological Society, 2003).

ONLINE METHODS

Plant materials and Fusarium head blight assays. The resistant and susceptible near-isogenic lines (R-NIL 260-1-1-2 and S-NIL 260-1-1-4) varying for the *Fhb1* interval of Sumai 3 on chromosome 3BS developed by Liu *et al.*[13] were used for expression analyses and as controls in all the experiments of the study. The NILs had been developed in two steps: first, a recombinant inbred line (RIL) population was developed by crossing Sumai 3 with Stoa, a susceptible cultivar[29]; then, a homozygous resistant RIL (RIL63) was crossed with another susceptible cultivar (MN97448), heterozygotes for the *Fhb1* interval were selected, and at the F_7 generation homozygous R- and S-NILs were isolated[13].

For association studies, seeds of 41 landraces and cultivars varying for *Fhb1* phenotype were provided by G. Bai of USDA-ARS unit located at Kansas State University. *Fusarium graminearum* isolate GZ 3639 was cultured in mung bean broth on a shaker at 30 r.p.m. kept at 25 °C for one week before the inoculations. This isolate has been well characterized for its high aggressiveness and DON production[17]. Macroconidia were counted on a hemocytometer as the average of the number of spores in four sections. Inocula were prepared by diluting the culture to a concentration of 1×10^5 spores/ml using sterile water. FHB inoculations were carried out in the Kansas State University greenhouses. We injected 10 µl of inoculum into a single floret of the tenth spikelet from the bottom of the spike at pre-anthesis, carefully avoiding any damage to other floral parts. The point of inoculation was marked with a black marker to monitor the spread of bleaching. The inoculated heads were covered with moisture-saturated Ziploc bags for 72 h to maintain humidity. Disease scores were taken 21 d after inoculation as the number of spikelets that were bleached downward from the point of inoculation. Percent disease severity (PDS) was calculated as number of bleached spikelets/total number of spikelets under the point of inoculation × 100. Plants with PDS above 40% were considered susceptible and below that were scored as resistant as has been done traditionally[17]. Mature seeds were threshed manually and analyzed for DON content.

BAC library screening, fingerprinting and construction of the physical map. A BAC library was developed from Sumai 3, a Chinese cultivar containing the *Fhb1* locus, with ~3× genome coverage and average insert size of ~100 kb. For library construction, genomic DNA was partially digested using the MboI restriction enzyme. DNA fragments in the 150–250 kb range were used in a ligation reaction with pIndigoBAC-5 linearized by BamHI (Epicentre). Ligated DNA was used for transformation of ElectroMax DH10B competent cells. To facilitate library screening, all BAC clones were arrayed onto high-density membranes, each containing 18,432 double-printed clones following the procedure described previously[30]. In addition, BAC library plate pools were prepared by combining 384 BAC clones from each plate followed by extraction of DNA by alkaline lysis method. All pools were normalized to 40 ng/µl for further screening. To construct a physical map of the Sumai 3 *Fhb1* region, 3BS markers from the corresponding region in Chinese Spring (**Supplementary Table 1**) were used to screen the BAC library using plate pools and high-density filters. Identified BACs were end-sequenced, and new markers were designed to further screen the library (**Supplementary Table 1**). DNAs of the selected BACs were extracted using Large-construct kit from Qiagen according to the manufacturer's instructions. Fingerprinting of the BACs was done by digesting each clone with a combination of 4-bp and 6-bp cutter restriction enzymes and separating fragments on 1.2% agarose gels following established protocols[31]. Eight BAC clones were found to span the majority of the region, out of which four constituted the minimum tiling path (476D8, 71I24, 383G12 and 572D13).

BAC sequencing and annotation. To sequence the *Fhb1* region of Sumai 3, four BAC clones were shotgun-sequenced using the Sanger approach. The sequence of the *Fhb1* region of Sumai 3 has been deposited in NCBI GenBank repository (KX907434). A total of ~2,300 Sanger paired-end sequence reads were obtained for each of these BAC clones. Sanger reads were assembled in contigs using the Consed, phred+phrap program. Additionally, BAC383G12 and BAC71I24 were sequenced using Ion Torrent PGM 316 sequencing system to fill the gaps in the assembly. Raw reads were quality trimmed and the initial assembly was performed within CLCBio (Qiagen) software environment. The assembly was then further filtered with minimum contig size of 300 bp, and minimum coverage of 50. The N50 of the assembly was 5 kb with an average length of 1.5 kb and with a total size of 125 kb. Sanger sequencing was performed to cover the gaps and resolve repetitive regions.

Gene annotation used the TriAnnot pipeline[32], F-GENESH (for *Triticum aestivum*), and GENSCAN (for maize) using default setting parameters. BLASTn and BLASTp searches in GenBank and Gene Ontology searches were done to predict the tentative function of the annotated genes. A total of 13 consensus confident gene predictions were made. All genes were resequenced using Sanger sequencing for high-confidence data.

Expression analyses. Expression analysis of the genes in the *Fhb1* region was carried out by inoculating the tenth spikelet from base rachis of S-NIL and R-NIL spikes at pre-anthesis stage with *Fusarium graminearum* macroconidia and water as control as described in FHB assays above. For collecting tissue for RNA extraction, the spikelets with the point of inoculation and the spikelets adjacent to it were cut quickly with a chilled pair of sharp scissors and flash frozen in liquid nitrogen 96 h after inoculations. The primers used for qPCR are provided in **Supplementary Table 1**. Actin was used as an internal control. The expression levels of the genes were calculated using the $2^{-\Delta CT}$ method and expressed as fold changes in *Fusarium graminearum* inoculated spikes relative to water inoculations.

Expression analysis of *PFT* was done in R-NIL and S-NIL 72 and 96 h after inoculation at the pre-anthesis stage with *F. graminearum* conidial suspension and water as mock control. Expression of *PFT* also was studied at various stages (pre-emergence, pre-anthesis, early anthesis, mid-anthesis, late anthesis and post-anthesis) of normal spike development. *PFT* gene expression also was studied in seedlings, leaves, stems and culms of the R-NIL plants, and the transcript levels were found to be much lower than that in the spikes (**Supplementary Fig. 2**).

RNA was extracted using TRIzol reagent (Thermo Fisher Scientific) using the manufacturer's protocol. Clean-up was done using RNeasy Mini Kit (Qiagen). Quantification was done using nanodrop and quality was checked using 2100 Bioanalyzer (Agilent Technologies). RNA samples with RIN values above 8 were used for qPCR studies. cDNA synthesis was done using High-Capacity cDNA Reverse Transcription Kit (Life Technologies) using the manufacturer's recommendations. Transcript levels of the candidate gene were determined by quantitative real-time PCRs (qRT-PCR) on a CFX96 Touch Real-Time PCR Detection System (Bio-Rad). The reactions were carried out in volume of 10 µl using iQ SYBR Green Supermix (Bio-Rad). Actin was used as an internal control. All samples had three biological replicates and were run in three technical replicates. Each qPCR was done in two copies.

5′ and 3′ rapid amplification of cDNA ends. RACE was done to determine the complete sequence of the *PFT* transcripts and identify the transcription initiation and termination sites. RACE was performed on RNA extracted from pre-anthesis spikes of R-NIL plants having an RNA integrity value above 9. The cDNA synthesis was done as described above. First Choice RLM-RACE kit (Thermo Fisher Scientific) was used on the cDNA to carry out 5′ and 3′ RACE using the manufacturer's instructions. The outer PCR of the 5′ RACE was performed with outer 5′ RACE primer supplied with the kit and 5′ RACE-PFT-Outer primer (**Supplementary Table 1**). The inner 5′ RACE products were generated using the kit 5′ RACE inner primer with 5′ RACE-PFT-Inner primer (**Supplementary Table 1**). The outer 3′ RACE PCR was done with the kit 3′ RACE outer primer and 3′ RACE-PFT-Outer primer (**Supplementary Table 1**), and further inner PCR was done on the products using inner 3′ RACE primer supplied with the kit and 3′ RACE-PFT-Inner primer (**Supplementary Table 1**).

PCR products from the 3′ RACE and 5′ RACE inner PCRs were purified with the QIAquick PCR purification kit (Qiagen). Purified fragments were subcloned into pCR2.1-TOPO (Life Technologies) and transformed into TOP10 One Shot Electrocomp *Escherichia coli* cells. A total of ten colonies were sequenced by the Sanger method using universal T3 and T7 primers, and the sequences were aligned to R-NIL genomic sequence to identify the transcription initiation and termination sites for *PFT*.

Screening and characterizing ethyl-methane sulfonate mutants. Seeds of the resistant, homozygous recombinant line HR58 (ref. 13) were mutagenized

doi:10.1038/ng.3706

with ethyl-methane sulfonate (EMS) according to Rawat *et al.*[33] with some modifications. Briefly, ~5,000 seeds were soaked in water for 8 h and treated with 0.5% EMS solution for 16 h at room temperature on a shaker at 100 r.p.m. Seeds were then washed under running tap water for 2 h and then grown in root trainers. Seeds were harvested at maturity and one M_2 seed per M_1 plant was advanced as a TILLING population with 2,267 individual plants. Among the M_2 plants, 1,929 were fertile and used for TILLING. DNA from all M_2 plants was extracted using a BioSprint kit (Qiagen), normalized to a concentration of 25 ng/µl and 4× pooled. The pools were screened for mutations in the candidate gene(s) using primers listed in **Supplementary Table 1** using Cel-1-based assay, following previously established protocols in our laboratory[33]. The identified mutant individuals were sequenced using the Sanger sequencing method. SNPs were identified by Clustal Omega alignment of reads with wild type HR58 and BAC383 amplified gene sequences. Additionally, the trace files were checked to confirm the SNPs identified. The identified missense mutations were analyzed for their SIFT and PROVEAN scores to predict their effect on the protein. Twenty-four M_3 plants of each identified mutant M_2 individual were grown and tested for homozygosity of the mutation and subsequent FHB evaluation as described above. **Supplementary Table 2** details the missense, nonsense and intronic mutants obtained and characterized for FHB phenotype.

DON content measurement of mutants and controls. The DON content of mutants after inoculation with *F. graminearum* was done at the Veterinary Diagnostic Laboratory at North Dakota State University, Fargo, by K. Benson according to established protocols[34]. Briefly, the seeds were crushed to a fine powder, and 1 g of each sample was extracted with acetonitrile/water while shaking. Five replicates of each sample were analyzed. The extracts were filtered and the eluents were evaporated. A mixture of TMSI (trimethylchlorosilane) and TMCS (*N*-trimethylsilyimidazole) was added to derivatize the sample. An internal standard was added, and the samples were separated by gas chromatography with electron capture detection (GC-ECD). All tests were run with three quality control pools.

RNAi-induced gene-silencing studies. An RNAi-based gene-silencing construct was made using the Gateway system described by Miki & Shimamoto[35]. The insert in the silencing construct consisted of a 306-bp sequence from exon 2 of *PFT*. The insert fragment was amplified from a cDNA pool synthesized from total RNA extracted from the spikes of R-NIL plants at pre-anthesis using the primers listed in **Supplementary Table 1**. The fragment was sub-cloned into a directional TOPO pENTER vector (pENTR Directional TOPO Cloning Kit, Thermo Fisher Scientific). The final RNAi-based silencing construct was made by recombination from an LR clonase reaction using a Gateway LR clonase enzyme mix (Life Technologies) between the entry vector carrying the *PFT* fragment and the pANDA-mini vector. Mini vector pANDA contains the maize (*Zea mays*) *ubi-1* promoter and the *nopaline synthase* terminator[35]. The RNAi construct contained the cDNA fragment derived from *PFT* oriented in the antisense and sense directions at the 5′ and 3′ ends of the construct, respectively, connected by a 1-kb GUS linker (**Fig. 3**).

RNAi lines were produced using particle-bombardment-mediated transformation of immature embryos of wheat cultivar Bobwhite as described[36]. The pANDA-mini vector was co-transformed with pHAC20 containing the herbicide-resistance *bar* gene as selectable marker in a 1:1 ratio[37]. Regeneration and selection of the transformed plants were performed as described[38]. The primers used for checking the presence of the *bar* gene and RNAi construct transformation events are provided in **Supplementary Table 1**.

Crosses were made between the R-NIL with RNAi Bobwhite. Reciprocal crosses also were made between the R-NIL and non-transformed Bobwhite. DNA was extracted from all F_1 plants, and PCR using primers GusF1 and pENTER-PFT-R (listed in **Supplementary Table 1**) was used to test the presence of RNAi construct. Five out of ten F_1 R-NIL-RNAi Bobwhite plants (Plants 1, 2, 6, 7 and 9) showed the presence of the RNAi construct. RNA was extracted and cDNA synthesized from spikes at pre-anthesis of F_1 plants from all the three types of crosses. Quantitative PCR was done to evaluate the extent of RNAi-induced gene silencing of *PFT* in the plants having RNAi construct using F_1 R-NIL-Bobwhite as a reference for comparison. Actin was used as an internal control. Each reaction was carried out in three technical replicates. For evaluating the phenotypic effect of gene silencing, spikes at pre-anthesis were inoculated along with R-NIL and Bobwhite as controls, and scored for FHB severity 21 d after inoculation as described in FHB assays above. Seeds were harvested at maturity.

Transformation of wheat with *PFT*. The 1,437-bp protein coding sequence of *PFT* was synthesized by GenScript USA Inc. and cloned into the pUC57 vector. Further, the coding sequence was subcloned into the pAHC17 vector[37] to drive expression by maize ubiquitin promoter. Immature embryos of wheat cultivars Bobwhite and Fielder were transformed with the construct using particle bombardment method[36]. Co-transformation was done with pHAC20 containing the herbicide-resistance *bar* gene as selectable marker in a 1:1 ratio[37]. Regeneration and selection of the transformed plants were performed as described previously[38]. Four primer pairs were used to check the presence of the *PFT* construct in the transformation events (**Supplementary Table 1**). Five independent T_0 events in Bobwhite (#7636, #7879, #7993, #7994 and #8328) and six T_0 events in Fielder (#7743, #7748, # 7872, #7977, #7978 and #8106) were obtained containing both transformed *PFT* gene and *bar* gene. The mRNA was extracted from the eleven T_0 plants as described before, and expression of transformed *PFT* was checked. Four out of 11 T_0 plants (#7636, #7879 and #7993 in Bobwhite, and #7978 in Fielder) were found to express the gene. The level of expression of *PFT* in all the positive T_0 events was found to be different (**Supplementary Fig. 4**). 15–20 T_1 plants from the 11 putative transgenic events were genotyped with the primers described above. Phenotyping was done by counting the number of diseased spikelets down from the point of inoculation at 11 d, 16 d and 21 d after inoculation with *F. graminearum* GZ3639 to monitor the rate of progress of the disease. At least three spikes were phenotyped for each plant. Area under disease progress curve (AUDPC) was calculated as described[39]. The four positive T_1 families (#7636, #7879, #7993 and #7978) co-segregated for the presence of transgene and resistance to FHB. Family #7879 in Bobwhite and #7978 in Fielder had healthy fertile plants similar to the untransformed control plants, and were checked for the expression of *PFT* as well as the FHB progress and severity (**Supplementary Table 7**). The plants from the same T_1 family showing expression of *PFT* were found to be either resistant or have a significantly slow progress of the disease, whereas those lacking the expression were highly susceptible like the untransformed controls (**Supplementary Fig. 5**).

Phylogenetic analyses. The phylogenetic analysis in **Supplementary Figure 7** was based on proteins similar to pore-forming toxin-like protein retrieved from NCBI database BLAST search with >35% sequence identity. Sequences were aligned with MUSCLE. Evolutionary analyses were conducted in MEGA6. Bootstrap confidence values were based on 100 iterations. The evolutionary distances were computed using the Poisson correction method. MEGA6 was used to generate the phylogenetic tree using a maximum-likelihood method. The NCBI and Uniprot accession numbers of all the proteins used are provided in **Supplementary Table 8**.

DON and D3G analyses. To test whether *PFT* plays a role in the detoxification of DON, two outer florets of the middle spikelet of spikes of the NILs, knockout mutant lines, and line HR58 were inoculated with purified DON provided by S. McCormick (USDA-ARS, Peoria, Illinois, USA). Ten µl of 10 µg/µl DON was applied between the lemma and palea of each floret. The inoculated spikes were covered with plastic bags for 3 d. The spikes were harvested at 1, 3, 7, 14 and 21 d after inoculation. For each line at every time point, six spikes were inoculated and two spikes were used as one sample or replication for DON and D3G test. The inoculated spikes were divided into three parts (apical, top third of the spike; middle, the inoculated and adjacent upper and lower spikelets; basal, bottom third of the spike) at the time of tissue collection to measure DON and D3G content in the parts of the inoculated spikes separately. Once the spikes were harvested, they were put in liquid nitrogen and then frozen at −80 °C. All the samples were freeze-dried before the DON and D3G tests.

The samples were analyzed according to Ovando-Martínez *et al.*[40] with a few modifications. The samples were extracted at 20:1 ratio of volume to weight with a acetonitrile:water mixture (84:16 v/v). The samples were shaken at 150 r.p.m. for 24 h at ~25 °C. The liquid extract was filtered through 0.2-µm nylon syringe filters into HPLC vials before analysis by UPLC-QTOF.

All filtered samples were stored at 4 °C until analysis. A series of standards also were prepared and analyzed with every set of samples. Matrix matched calibration standards were prepared at several concentrations for DON and D3G to take into consideration any matrix effects from compounds extracted from wheat. The concentrations of DON standards used were 20.0, 10.0, 6.0, 4.0, 2.0, 1.0, 0.7, 0.5, 0.2 and 0.1 p.p.m., and the D3G standards were 10.0, 5.0, 3.0, 2.0, 1.0, 0.5, 0.35, 0.25, 0.1, and 0.05 p.p.m. The DON extracted ion chromatogram used the mass-to-charge ratio of the $(M+H)^+$ ion (297.1333), and the D3G EIC used the mass-to-charge ratio of the $(M+Na)^+$ ion (481.1680).

Protein structure prediction and comparison. The protein structure for the predicted *PFT* gene product was modeled and proteins with the most homologous structures were identified using the default settings of Phyre2 (ref. 41). The top scoring model identified, with 100% confidence, similarity of 33% was agglutinin. The ETX pore-forming toxin domain was also predicted with 100% confidence and 19% identity. Other high-scoring models gave similar results, suggesting that this gene may participate in identification of fungal carbohydrates and arresting the growth of the fungus.

29. Waldron, B.L., Moreno-Sevilla, B., Anderson, J.A., Stack, R.W. & Frohberg, R.C. RFLP mapping of QTL for *Fusarium* head blight resistance in wheat. *Crop Sci.* **39**, 805–811 (1999).
30. Akhunov, E.D., Akhunova, A.R. & Dvorák, J. BAC libraries of *Triticum urartu*, *Aegilops speltoides* and *Ae. tauschii*, the diploid ancestors of polyploid wheat. *Theor. Appl. Genet.* **111**, 1617–1622 (2005).
31. Mathewson, C.A., Schein, J.E. & Marra, M.A. Large-scale BAC clone restriction digest fingerprinting. *Curr. Protoc. Hum. Genet.* **53**, 5.19 (2007).
32. Leroy, P. *et al.* TriAnnot: a versatile and high performance pipeline for the automated annotation of plant genomes. *Front. Plant Sci.* **3**, 5 (2012).
33. Rawat, N. *et al.* A diploid wheat TILLING resource for wheat functional genomics. *BMC Plant Biol.* **12**, 205 (2012).
34. Tacke, B.K. & Casper, H.H. Determination of deoxynivalenol in wheat, barley, and malt by column cleanup and gas chromatography with electron capture detection. *J. AOAC Int.* **79**, 472–475 (1996).
35. Miki, D. & Shimamoto, K. Simple RNAi vectors for stable and transient suppression of gene function in rice. *Plant Cell Physiol.* **45**, 490–495 (2004).
36. Finer, J.J., Vain, P., Jones, M.W. & McMullen, M.D. Development of the particle inflow gun for DNA delivery to plant cells. *Plant Cell Rep.* **11**, 323–328 (1992).
37. Christensen, A.H. & Quail, P.H. Ubiquitin promoter-based vectors for high-level expression of selectable and/or screenable marker genes in monocotyledonous plants. *Transgenic Res.* **5**, 213–218 (1996).
38. Saintenac, C. *et al.* Identification of wheat gene *Sr35* that confers resistance to Ug99 stem rust race group. *Science* **341**, 783–786 (2013).
39. Madden, L.V., Hughes, G. & van den Bosch, F. *The Study of Plant Disease Epidemics* (American Phytopathological Society, 2007).
40. Ovando-Martínez, M. *et al.* Analysis of deoxynivalenol and deoxynivalenol-3-glucoside in hard red spring wheat inoculated with *Fusarium graminearum*. *Toxins (Basel)* **5**, 2522–2532 (2013).
41. Kelley, L.A. & Sternberg, M.J.E. Protein structure prediction on the Web: a case study using the Phyre server. *Nat. Protoc.* **4**, 363–371 (2009).

doi:10.1038/ng.3706